



# Co-pyrolysis of macroalgae and lignocellulosic biomass

## Synergistic effect, optimization studies, modeling, and simulation of effects of co-pyrolysis parameters on yields

Benjamin Bernard Uzoejinwa<sup>1,2</sup> · Xiuhua He<sup>1</sup> · Shuang Wang<sup>1</sup> · Abd El-Fatah Abomohra<sup>1,3</sup> · Yamin Hu<sup>1</sup> · Zhixia He<sup>1</sup> · Qian Wang<sup>1</sup>

Received: 31 May 2018 / Accepted: 13 October 2018 / Published online: 27 October 2018  
© Akadémiai Kiadó, Budapest, Hungary 2018

### Abstract

Synergistic effect of co-pyrolysis of macroalgae [*Enteromorpha prolifera* (EP)] and lignocellulosic biomass [rice husk (RH)] in a fixed bed reactor for maximum and enhanced biofuels yield has been investigated. The main and interaction effects of three effective co-pyrolysis parameters (*pyrolysis temperature, feedstock blending ratio, and heating rate*) were also modeled and simulated to determine the yield rates of bio-oil and bio-char, respectively. Optimization studies were, then, performed to predict the optimal conditions for maximum yields using the central composite circumscribed experimental design in Design Expert<sup>®</sup> software 8.0.6. Analysis of variance was carried out to determine whether the fit of the multiple regressions is significant for the second-order model. Normal pyrolysis oils from EP, RH, and co-pyrolysis oils obtained from different feedstock blending ratios were examined using the gas chromatography-mass spectrometry to identify their compositions. Some vital properties of oils and bio-chars such as the *heating value, water content, elemental compositions, and specific gravity* were also determined, which unveiled that synergistic effect exists between EP and RH during co-pyrolysis, and this led to increase in products' yields and improved co-pyrolysis products' quality.

**Keywords** Co-pyrolysis · Macroalgae · Lignocellulosic biomass · Synergistic effect · Increased/enhanced products' yields

### Introduction

In recent years, biofuels have attracted a considerable attention [1–3] as the struggle with identifying renewable replacements for fossil fuels and other forms of conventional energy sources in the world still persists. Biofuels can be solid, liquid, or gaseous in nature and are mainly

produced from the biomass, and these important products include, among others, bio-oil, bioethanol, biobutanol, biodiesel, biomethane, biohydrogen, bio-crude, biogas, bio-char, and hydrochar [4]. In order to reduce the contribution to global environmental warming and pollution due to overconsumption of fossil fuels owing to rapid economic development and population expansion, it is important to develop, optimize, and utilize biomass energy, the fourth largest energy system after coal, oil, and gas, supplying approximately 14% of the world annual energy consumption [5].

Algal biomass, most especially the macroalgae (seaweed), has been recognized as a promising energy source for the third-generation biofuels [6]. Seaweed biomass resource is abundant because of the extensive adjacent oceans, seas, and other water bodies, almost across the Universe. Besides its availability and the absence of direct competition for agricultural land and crop production [7], seaweed also has high photosynthetic efficiency, fast

✉ Xiuhua He  
xiuhua.he@ujs.edu.cn

✉ Shuang Wang  
alexjuven@ujs.edu.cn

<sup>1</sup> School of Energy and Power Engineering, Jiangsu University, Zhenjiang 212013, Jiangsu, China

<sup>2</sup> Department of Agricultural and Bioresources Engineering, University of Nigeria, Nsukka 41001, Enugu State, Nigeria

<sup>3</sup> Botany Department, Faculty of Science, Tanta University, Tanta 31527, Egypt

growth reproduction rate, strong adaptability, ability to fix CO<sub>2</sub> to organic substances [8], high economic and environmental benefits [5], and is easy to cultivate. The chemical compositions of the seaweed mainly include fatty compounds, soluble polysaccharides, and proteins [9, 10], which are easy to be pyrolyzed. The compositions of macroalgae are different from the pyrolysis properties of the terrestrial lignocellulosic biomass, like the rice husk, that are composed of cellulose, hemicellulose, and lignin. In addition, the lignocellulosic biomass is a carbon-neutral and renewable resource with abundant reserves that about 220 billion tons of the dry biomass could be produced worldwide every year [1, 5, 11].

Generally, the recycling of energy from wastes, most especially, the agricultural and organic wastes, has received increasing interests in recent years, and a variety of methods have been developed [12–18], and among them, pyrolysis represents an effective thermo-chemical conversion process for both waste disposal and energy recovery [5, 19–22]. Pyrolysis of nuisance and residual algal biomass such as seaweeds, with the terrestrial lignocellulosic biomass like the rice husk for bioenergy production, is therefore a promising process for renewable fuels production. Many researchers have made a thorough research on the normal pyrolysis of rice husk [14, 23–26]. Also, many normal pyrolysis studies have focused on oil production from algal biomass because they are considered as abundant and promising renewable energy sources [19, 27]. Meanwhile, the normal pyrolysis of macroalgae (seaweeds) was discovered to be exothermic [28], while that of lignocellulosic biomass needs to absorb heat [29]. However, the utilization of the bio-oil produced from the normal pyrolysis process has been limited due to some drawbacks such as high oxygen and water contents, low heating value, and instability [30]. It is thus of great importance to find effective solution for improving the biomass's normal pyrolysis products. The co-pyrolysis of biomass with other organic wastes, other types of biomass or synthetic polymers, seems to be a simple and effective way for such improvement, not only in products' yield but also in quality [5, 31]. Different biomass and organic wastes usually have different chemical and physical properties such as moisture, volatile matter, ash content, calorific value, porosity, and oxygen/hydrogen/carbon (O/H/C) molar ratios. The differing properties can change the reactivity and thermal characteristics of samples and products, and the formation of synergistic interaction during co-pyrolysis could then result in improved pyrolysis products [32, 33]. Co-pyrolysis shows synergistic effect and is considered more economical; hence, it is regarded as an effective technique for bio-oil upgrading [1, 5, 34].

Numerous efforts have been made in investigating the co-pyrolysis of biomass with other wastes, such as waste

tyres [35]; coal [29]; synthetic polymers/plastics [36]; and sewage sludge [37]. However, so far there has been very limited research works investigating the co-pyrolysis of macroalgal biomass with organic wastes or other biomass [1, 33, 38]. As a result, this present study investigated the co-pyrolysis of a typical macroalgae [*Enteromorpha prolifera* (EP)] with lignocellulosic biomass [rice husk (RH)] in a fixed bed reactor. It also modeled and simulated the main and interaction effects of three effective co-pyrolysis parameters (*pyrolysis temperature, heating rate, and feedstock blending ratio*) on the products' yields using central composite circumscribed experimental design in Design Expert<sup>®</sup> 8.0.6 software [12, 34, 39]. Also, optimization studies were performed to predict the optimal conditions for maximum co-pyrolysis products' yields [5]. The synergistic effects on the yield and quality of co-pyrolysis products were also analyzed in terms of the heating values, products' yields, and other characteristics. The results of the products' analysis unveiled the extent to which the synergistic effect that exists between EP and RH during co-pyrolysis has enhanced the products' yield and quality. The results of this present study would also provide valuable information for developing an effective strategy in terms of both resource recycling and organic waste management.

## Materials and methods

### Materials and analysis

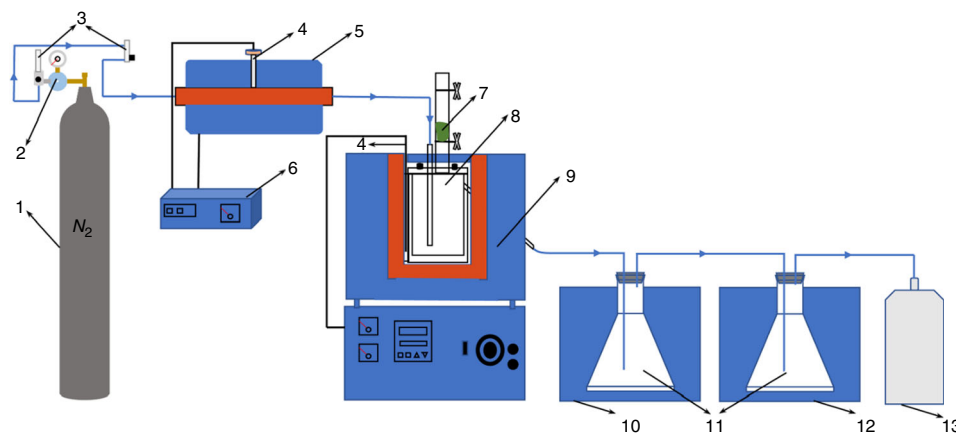
In this present study, the feedstock materials used include macroalgae [*Enteromorpha prolifera* (EP)], a typical green seaweed, and terrestrial lignocellulosic biomass [rice husk (RH)], which is also a common agricultural residue. These samples were dried and stored in a cool and dry environment. Then, the dried materials were ground by a pulverizer into particles of size 0.18–0.45 mm. The proximate and ultimate analysis results of the individual feedstocks and their mixture are presented in Table 1.

### Pyrolysis process procedures

Pyrolysis experiments of individual EP, RH, and their mixtures were performed in a fixed bed reactor, as shown in Fig. 1. The fixed bed reactor (internal diameter 70 mm, height 100 mm) was heated with electric resistance wire, with programed temperature controller. A thermocouple sensor was inserted into the reactor to record the temperature change. The sweeping nitrogen gas was passed through the tube furnace into the reactor at a constant flow rate of 100 mL min<sup>-1</sup> to ensure an inert atmosphere and effective residence time of pyrolysis volatile. Samples were

**Table 1** Proximate and ultimate analysis of samples

Material	Proximate analysis/mass% (ad)				Ultimate analysis/mass% (ad)					LHV/MJ kg <sup>-1</sup>
	A	V	FC	M	C	H	O	N	S	
EP	28.56	53.95	10.69	6.80	29.42	3.96	21.76	7.05	2.45	14.01
RH	11.41	61.99	16.00	10.60	40.20	4.68	31.77	1.20	0.14	17.67
EP:RH	18.67	56.17	15.16	10.00	34.81	4.32	26.77	4.13	1.30	16.43

**Fig. 1** Schematic diagram of the fixed bed co-pyrolysis apparatus. 1. Nitrogen cylinder; 2. gas pressure gauge; 3. flowmeter; 4. thermocouple; 5. N<sub>2</sub> preheating equipment; 6. controller; 7. algae sample; 8. fixed bed reactor; 9. furnace; 10. condenser (I); 11. bio-oil storage; 12. condenser (II); 13. gas bag

1. Nitrogen cylinder; 2. Gas-pressure gauge; 3. Flowmeter; 4. Thermocouple; 5. N<sub>2</sub> preheating equipment; 6. Controller; 7. Algae sample; 8. Fixed bed reactor; 9. Furnace; 10. Condenser (I); 11. Bio-oil storage; 12. Condenser (II); 13. Gasbag

heated to the set temperature at a given heating rate as shown in Table 2. Besides, the asbestosed wire gauze was used to filter the char at the exit of volatiles and non-condensable gas. During the experiments, two condensers were applied as shown in Fig. 1 to convert the condensable volatiles to liquid form. The pyrolysis was performed with 5 g of the feedstock based on the experimental design's feed ratios (Table 2), at 100 mL min<sup>-1</sup> nitrogen gas flow rate. After each pyrolysis process, the liquid oil product was collected from condensers and weighed, and the mass of char produced determined. The percentage yields of pyrolytic liquid and char for all the experiments were calculated using the following equation [34]:

$$\text{Yield of product} = \frac{\text{Desired product}}{\text{Total feed}} \times 100\% \quad (1)$$

while the gas yield was determined by overall mass balance. The theoretical products' yields of co-pyrolysis of EP with RH were calculated as follows:

$$Y_{\text{theoretical yield}} = \alpha \times Y_{\text{EP}} + \omega \times Y_{\text{RH}} \quad (2)$$

where  $Y_{\text{theoretical yield}}$  is the theoretical product yield of the co-pyrolysis;  $Y_{\text{EP}}$  and  $Y_{\text{RH}}$  represent the yields from the individual pyrolysis of seaweed (EP) and rice husk (RH) under the same experimental conditions of co-pyrolysis, respectively;  $\alpha$  and  $\omega$  represent the mass percentages (%) of EP and RH in the feedstock, respectively. The

synergistic effect of co-pyrolysis was evaluated by comparing the theoretical yields with the actual yields, and validation experiments were performed to compare the sum of the yields from individual pyrolysis of EP and RH with that from the co-pyrolysis of EP and RH, however, together with a selected additional 40% of RH. Each experimental treatment had five replicates, and the statistical difference between the sum of yields from individual pyrolysis and those from the co-pyrolysis was evaluated. The amount of EP and RH used in the individual pyrolysis was the same as that of each material employed in the co-pyrolysis.

### Experimental design and optimization study

In this study, three experimental factors: rice husk (RH) mass percentage in the feedstock, pyrolysis temperature, and heating rate were investigated. A five level, three variable, central composite circumscribed (CCC) experimental design method, which has a factorial design and star points at a distance of  $\pm 1.682$  from the central point, was employed for arranging the co-pyrolysis experiments using Design Expert<sup>®</sup> 8.0.6. Therefore, a total of 17 experimental runs (consisting of eight factorial points, three center points, and six star points) are required using the CCC experimental design method. Each experiment arranged at the center of experimental domain (i.e., experimental runs 15–17) was repeated for three times in order to estimate the

**Table 2** An array of the CCC design for co-pyrolysis experiments and product yields

Runs	Factors (independent variables)			Response	Response	Other co-pyrolysis product
	RH % in the feedstock <sup>a</sup> /mass%	Temperature <sup>a</sup> /°C	Heating rate <sup>a</sup> /°C min <sup>-1</sup>	1/mass% Bio-oil yield	2/mass% Char yield	yields/mass% Gas yield
1	(- 1)20	(- 1)450	(- 1)10	40.2	28.8	31.0
2	(+ 1)80	(- 1)450	(- 1)10	45.5	24.5	29.9
3	(- 1)20	(+ 1)550	(- 1)10	41.6	28.4	30.0
4	(+ 1)80	(+ 1)550	(- 1)10	45.3	24.5	29.2
5	(- 1)20	(- 1)450	(+ 1)20	42.9	28.4	28.7
6	(+ 1)80	(- 1)450	(+ 1)20	47.2	21.5	30.6
7	(- 1)20	(+ 1)550	(+ 1)20	42.5	28.1	29.4
8	(+ 1)80	(+1)550	(+ 1)20	46.2	22.8	31.0
9	(- 1.682)0	(0)500	(0)15	39.2	31.4	29.4
10	(+ 1.682)100	(0)500	(0)15	46.8	24.0	31.2
11	(0)50	(- 1.682)400	(0)15	43.6	25.0	31.4
12	(0)50	(+ 1.682)600	(0)15	44.3	25.9	29.8
13	(0)50	(0)500	(- 1.682)5	43.2	27.5	29.3
14	(0)50	(0)500	(+ 1.682)25	45.9	24.1	30.0
15	(0)50	(0)500	(0)15	45.2	24.2	30.6
16	(0)50	(0)500	(0)15	45.5	23.1	31.4
17	(0)50	(0)500	(0)15	45.2	23.4	31.4

<sup>a</sup>Coded levels (in parentheses) and real values of experimental factors

pure error. The experimental data were statistically analyzed using the analysis of variance (ANOVA) method, while the multiple linear regression analysis was performed to fit a quadratic polynomial model:

$$Y = \beta_0 + \sum_{i=1}^3 \beta_i X_i + \sum_{i=1}^3 \beta_{ii} X_i^2 + \sum_{i=1}^3 \sum_{j=i}^2 \beta_{ij} X_i X_j \quad (3)$$

where  $Y$  (which can be either  $Y_{\text{bio-oil}}$  or  $Y_{\text{char}}$ ) is the response variable (for pyrolysis oil and bio-char yields, respectively);  $X_i$  or  $X_j$  is the independent variable (i.e., experimental factor);  $\beta_0$ ,  $\beta_i$ ,  $\beta_{ii}$ , and  $\beta_{ij}$  are the intercept, linear, quadratic, and interaction coefficients of the model, respectively. The experimental factors are denoted in this study by the following symbols:  $A$  represents the mass percentage of rice husk (RH) in the feedstock (%),  $B$  depicts the pyrolysis temperature (°C), and  $C$  denotes the heating rate (°C min<sup>-1</sup>). The pyrolysis oil and char yields were thus evaluated as the sum of a constant, three first-order effects (i.e., terms in  $A$ ,  $B$ , and  $C$ ), three interaction effects (i.e.,  $AB$ ,  $AC$ , and  $BC$ ), and 3 s-order effects ( $A^2$ ,  $B^2$ , and  $C^2$ ), respectively, based on Eq. (3). Only the terms that are statistically significant were used in the development of the models. The optimal co-pyrolysis conditions for maximum bio-oil yield and minimum char yield were then identified using the numerical optimization function of

Design Expert<sup>®</sup> software 8.0.6. The experimental levels (coded as  $\pm 1$ , 0, and  $\pm 1.682$ ) and their real values are presented in Table 2.

During the optimization study process, the desirability functions, based on the nature of the objective of each response which can be ‘to minimize’, ‘to maximize’, ‘target’, ‘in range’, or ‘equal to’, are useful in determining the balanced or optimum settings for each of the responses. Thus, in this present study, the objective is to maximize the bio-oil yield (i.e., the first response) and to minimize the bio-char yield (i.e., the second response), consecutively. Under the maximization approach when the target value for the response,  $Y_{\text{bio-oil}}$ , is a maximum, each  $i$ th response is assigned a desirability function,  $d_i$ , whose values vary between 0 and 1, and is defined based on the objective of the response as follows:

$$d_i = \begin{cases} 0 & \text{if } Y_i < L \\ \left( \frac{Y_i - L}{T - L} \right)^\omega & \text{if } L \leq Y_i \leq T \\ 1 & \text{if } Y_i > T \end{cases} \quad (4)$$

where  $T$  is the target value of the  $i$ th response,  $Y_i$ ,  $L$  denotes the acceptable lower limit value for the response, and  $\omega$  is the mass. When  $\omega = 1$ , the desirability function is linear. If  $\omega > 1$ , then more importance is placed on achieving the target for the response,  $Y_i$ , but if  $\omega < 1$ , less mass is

assigned to achieve the target for the response,  $Y_i$ . The masses normally provide more emphasis on the upper and lower bounds. Once a desirability function is defined for each of the responses, assuming that there are ‘ $m$ ’ responses, the individual desirability values of each response are then combined using geometric mean to obtain an overall desirability objective function,  $D$ , that varies over  $0 < D < 1$ , as follows:

$$D = (d_1^{T_1} \cdot d_2^{T_2} \dots d_m^{T_m})^{1/(r_1+r_2+\dots+r_m)} \quad (5)$$

where the  $T_i$  represents the importance of each response and the greater the value of  $T_i$ , the more important the response with respect to the other responses.

However, in the case of minimization approach when the target value for the response,  $Y_{\text{bio-char}}$ , is a minimum, each  $i$ th response is assigned a desirability function,  $d_i$ , whose values vary between 1 and 0, and is defined based on the objective of the response as follows:

$$d_i = \begin{cases} 1 & \text{if } T < Y_i \\ \left(\frac{U - Y_i}{U - Y_i}\right)^\mu & \text{if } T \leq Y_i \leq U \\ 0 & \text{if } Y_i > U \end{cases} \quad (6)$$

where  $U$  denotes the acceptable upper limit value to the response, and  $\mu$  is the same as the mass used to attribute levels of importance to the target value just as  $\omega$ . But if the target value ( $T$ ) is located between the lower limit ( $L$ ) and the upper limit ( $U$ ), then a bilateral desirability function is applied and it is given by:

$$d_i = \begin{cases} 0 & \text{if } Y_i < L \\ \left(\frac{Y_i - L}{T - L}\right)^\omega & \text{if } L \leq Y_i \leq T \\ \left(\frac{U - Y_i}{U - Y_i}\right)^\mu & \text{if } T \leq Y_i \leq U \\ 0 & \text{if } Y_i > U \end{cases} \quad (7)$$

### Analysis of bio-oil and char products and determination of some vital oil and char properties

GC-MS analysis was carried out on the bio-oils obtained from the pyrolysis of the individual samples and their mixtures at different blending ratios, respectively. In addition, some important properties of the bio-oils and char were determined using the American Society for Testing and Materials (ASTM) methods: the specific gravity (ASTM D4052), the higher heating value (ASTM D240), and water content (ASTM E203).

## Results and discussion

### Sample analysis results

Table 1 presents the proximate and ultimate analyses of the individual feedstocks (EP, RH) and their mixture, at a feed ratio of 1:1, carried out by a Costech<sup>®</sup> ECS 4010 elemental analyzer according to American Society for Testing and Materials (ASTM) methods.

### Pyrolysis oil and char yields

Table 2 presents the oil and char yields of varying quantity and quality, as well as the gaseous products obtained from the pyrolysis of EP and RH under different operating conditions and feedstock blending ratios. From the table, it can be observed that the oil yield from the normal pyrolysis of EP and RH alone is 39.2 mass% (i.e., at run #9) and 46.8 mass% (at run #10), respectively. Thus, the normal pyrolysis of RH alone produced more bio-oil than that of EP, probably because RH contains higher volatile matter. However, the ultimate analysis results showed that RH has higher oxygen content than EP (Table 1). It was also noticed that the normal pyrolysis of EP alone produced more char (31.4 mass%) than that of RH (24 mass%) under the same pyrolysis operating conditions of *temperature* (500 °C) and *heating rate* (15 °C min<sup>-1</sup>) (Table 2). This could be probably because the EP has more ash content than the RH (Table 1). It is worth noting that a higher bio-oil yield of 47.2 mass% was recorded from the co-pyrolysis with 20% of EP and 80% of RH during the fixed bed reactor experiments at 450 °C with a *heating rate* of 20 °C min<sup>-1</sup> (i.e., at run #6). This result indicated the existence of a synergistic effect during the co-pyrolysis. Similarly, the lowest bio-char yield of 21.5 mass% was obtained under the same co-pyrolysis conditions for the higher oil yield. It was also observed that the co-pyrolysis of seaweed with rice husk led to a significant reduction in the production of bio-char when compared to the bio-char produced from normal pyrolysis of seaweed alone. The results of the fixed bed reactor experiments were then used to model and simulate the oil and char yield rates, respectively, using the Design Expert<sup>®</sup> software 8.0.6.

### Model fitting, evaluation, and ANOVA analysis

Mathematical models were developed by fitting a second-order polynomial function for the response data (bio-oil and char yields, respectively) as specified by Eq. (3). Thus, the main and interaction effects of the three effective experimental factors: (*the pyrolysis temperature, feedstock blending ratio, and heating rate*, denoted as A, B, and C)

were modeled using the response surface method. The results of the models revealed that both the main and interaction effects of A, B, and C were significant for both oil and char yields, respectively. Thus, the regression models for the bio-oil and char yield rates are presented as follows:

$$Y_{\text{bio-oil}} = 44.9 - 2.24A + 0.282 \times 10^3 B + 0.848C - 0.427AB - 0.0331AC - 0.438BC - 0.801A^2 - 0.470B^2 - 0.145C^2 \quad (8)$$

$$Y_{\text{bio-char}} = 24.0 - 2.15A + 0.0743B - 1.16C + 0.295AB - 0.442AC + 0.186BC + 1.42A^2 + 0.644B^2 + 0.432C^2 \quad (9)$$

The coefficient of determination ( $R^2$ ) can be used to verify the precision of a model [39]. In this study, the  $R^2$  values for the responses (oil and char yields) were determined as 0.993 and 0.986, respectively, which are very close to unity, and these implied that the sample variations of 99.3% and 98.6% for the oil and char responses, respectively, were attributed to the independent variables, and only about 0.7% and 1.4% of the total variations, respectively, cannot be explained by the models (Table 3). These results showed that the accuracy and ability of the models for predictions are relatively high and the predicted  $R^2$  values of 0.946 and 0.928 (for oil and char yields) are in good agreement with their adjusted  $R^2$  values of 0.985 and 0.969, respectively. The determined model evaluation parameters advocated a high correlation between the observed and predicted values in this present work.

Generally, a high value of predicted  $R^2$  value indicates that the developed model can be used as a predictive tool over the whole parameter uncertainty range. Likewise, the lack of fit was not significant ( $P > 0.05$  for both cases) relative to the pure error, which implies that the models are also robust. Also, adequate precision normally measures the signal-to-noise ratio, and a precision ratio greater than 4 is said to be desirable and adequate. Thus, in this present study, the precision ratios of 38.2 and 27.2 were obtained for the responses (oil and char yields), respectively, and this indicated adequate signals and suggested that the models can be used to navigate the design space. In order to validate the developed models, ANOVA (analysis of variance) was used to determine whether the fits of the multiple regressions are significant for the second-order model. The results of the ANOVA are presented in Table 4a, b, for oil and char yields, respectively. The statistical significance of the developed models was determined by using the  $F$  test. Probability values ( $P$  values) were used to verify the significance of each factor on the oil

and char yields, consecutively. According to Yi et al. [39], the smaller the  $P$  value, the more significant the corresponding factor. The models were found to be significant at 5% confidence level ( $P < 0.05$ ) based on the  $F$  test.

The normal probability plots were used to verify the distribution of residuals and normality assumption for the measured data (bio-oil and char yields). Figure 2a, b presents the normal probability plot of residuals for bio-oil and char yields, respectively. This indicated that the residuals for the oil and char yields followed a normal distribution, as they fell on or within a straight line showing that errors are distributed normally. This is thus one of the basic statistical conditions for the validity of the analysis of variance (ANOVA) besides the plot of the residuals versus the actual responses as shown in Fig. 3a, b, respectively. This revealed that the predicted responses' values are in good agreement with their actual values in the range of the operating variables. While Fig. 4a, b presents the plot of the residuals versus the predicted responses (bio-oil and char yields, respectively) which revealed that the residuals scattered randomly on the display, this indicates that the proposed models are adequate and the assumptions of the independence or constant variance are not violated [39, 40].

## Optimization study results, confirmatory experiments, and the effects of factors on responses

### The bio-oil yields

The optimal conditions for maximum production of pyrolysis oil (bio-oil) were obtained from the optimization study as a *pyrolysis temperature* of 455 °C and *heating rate* of 20 °C min<sup>-1</sup> with 80% mass of RH in the feedstock blend which gave the maximum predicted bio-oil yield of 47.70 mass% (Fig. 5a). The result of the statistical analysis revealed that the feedstock ratio (i.e., RH mass percentages in the feedstock mixture), pyrolysis temperature, and heating rate significantly influenced the bio-oil yields from the co-pyrolysis of seaweed (EP) with rice husk (RH). In order to validate the model's prediction, the results of three confirmatory experimental tests that were conducted in the fixed bed reactor under the same predicted optimal conditions gave 48.20 mass%, 48.05 mass%, and 47.90 mass% of bio-oil yields, respectively, compared to the predicted optimal bio-oil yield of 47.70 mass% (Table 5). It was also observed that the percentage errors in prediction for the response (i.e., the bio-oil yield measured at the optimal co-pyrolysis conditions) varied from 0.42 to 1.04% (Table 5). This implied that the model's prediction is accurate. Moreover, many researchers reported in the literature that the maximum oil yield from the pyrolysis of biomass often

**Table 3** Model evaluation parameters

Parameters	Values for each response model evaluation	
	Bio-oil	Char
$R^2$	0.993	0.986
$R^2$ adjusted	0.985	0.969
$R^2$ predicted	0.946	0.928
$P > F$	< 0.0001	< 0.0001
SD	0.286	0.473
Coefficient of variance/%	0.648	1.85
Mean	44.2	25.6
PRESS	4.69	8.32
Adequate precision	38.2	27.2

*PRESS* predicted residual sum of squares

**Table 4** ANOVA results for (a) bio-oil yields, (b) bio-char yields

Source of variation	Sum of squares	Degree of freedom	Mean square	<i>F</i> value	<i>P</i> value	Prob. > <i>F</i>
(a)						
Model	87.1	9	9.67	118	< 0.0001	Significant
<i>A</i> -Feedstock ratio	48.6	1	48.6	593	< 0.0001	
<i>B</i> -Temperature	0.602	1	0.602	7.34	0.0303	
<i>C</i> -Heating rate	8.00	1	8.00	97.6	< 0.0001	
<i>AB</i>	1.05	1	1.05	12.8	0.00897	
<i>AC</i>	0.0112	1	0.0112	0.137	0.0422	
<i>BC</i>	1.36	1	1.36	16.6	0.00472	
$A^2$	6.72	1	6.72	81.9	< 0.0001	
$B^2$	2.19	1	2.19	26.7	0.00131	
$C^2$	0.659	1	0.659	8.03	0.0253	
Residuals	0.574	7	0.0820	–	–	–
Lack of fit	0.514	5	0.103	3.43	0.241	Not significant
Pure error	0.0600	2	0.0300	–	–	–
Cor. Total		16	–	–	–	–
(b)						
Model	113	9	12.6	56.3	<0.0001	Significant
<i>A</i> -Feed ratio	44.6	1	44.6	200	<0.0001	
<i>B</i> -Temperature	0.0417	1	0.0417	0.186	0.0479	
<i>C</i> -Heating rate	15.1	1	15.1	67.4	<0.0001	
<i>AB</i>	0.500	1	0.500	2.24	0.0178	
<i>AC</i>	2.00	1	2.00	8.95	0.0202	
<i>BC</i>	0.245	1	0.245	1.10	0.0330	
$A^2$	21.2	1	21.2	94.8	<0.0001	
$B^2$	4.09	1	4.09	18.3	0.00366	
$C^2$	5.82	1	5.82	26.0	0.00140	
Residuals	1.56	7	0.224	–	–	–
Lack of fit	0.918	5	0.184	0.568	0.736	Not significant
Pure error	0.647	2	0.323	–	–	–
Cor. Total		16	–	–	–	–

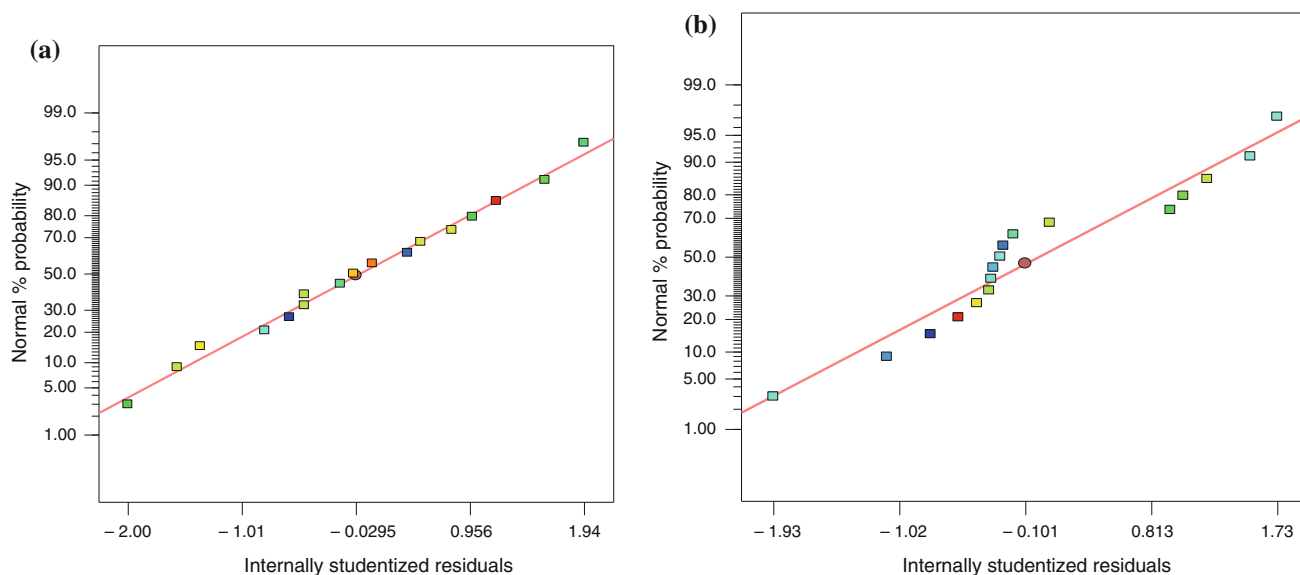


**Fig. 2** Normal probability plots of residuals for: **a** bio-oil and **b** char yields, respectively

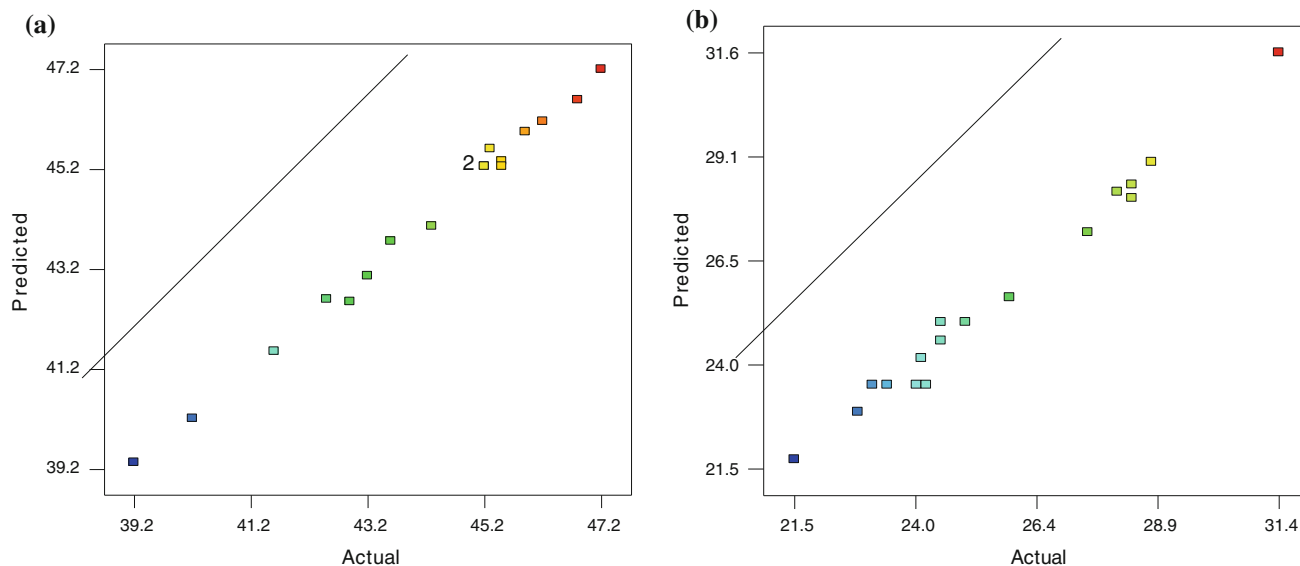


**Fig. 3** Graphs of the predicted values versus the actual values for: **a** bio-oil and **b** char yields, respectively

occurred in the temperature range of 450–550 °C [15, 19, 20, 34, 41]. The result of the optimal co-pyrolysis temperature, in this present study, was found to be consistent with that observation. Concurrently, Fig. 5 presents the simulated main effects of the individual factors and those of their interaction effects on the pyrolysis oil yield rates. Considering the simulated main effects of the individual factors investigated, it was observed that the bio-oil yield rate increases with an increasing mass percentage of RH in the feedstock mixture until a maximum oil peak of 47.70 mass% was obtained with 80% of RH in the feedstock mixture, after which there was a slight continuous decline in the oil yield as the mass percentage of RH in the

mixture further rises (Fig. 5a). Likewise, a maximum bio-oil yield of 48.20 mass% was obtained during the laboratory confirmatory test experiments in a fixed bed reactor that were conducted under the same predicted optimal conditions. This peak yield of bio-oil could be traced to the synergistic interactions that exist between EP and RH during co-pyrolysis process, probably due to the apparent differences in both their individual compositions and thermal decomposition behaviors [1]. This result indicated that the addition of RH to EP during pyrolysis can serve as a suitable blend for improving both the yield and quality of products obtained from the process [28, 29]. Likewise, the *pyrolysis temperature* significantly influenced the bio-oil



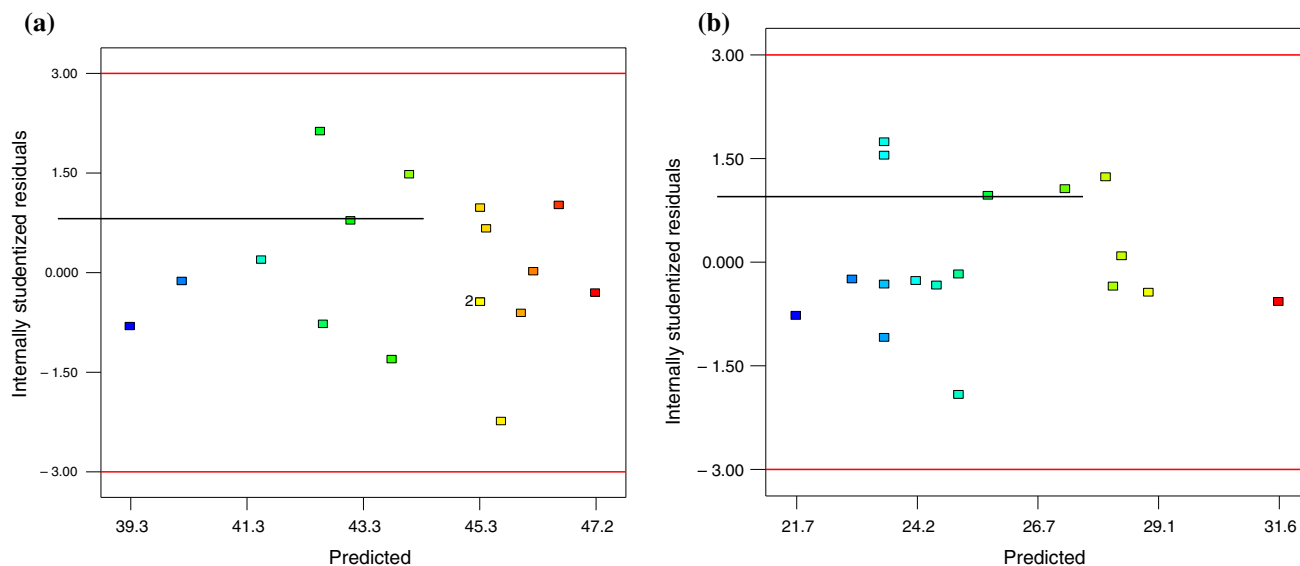


**Fig. 4** Plots of residuals versus predicted values for: **a** bio-oil and **b** char yields, respectively

yield rates. The bio-oil yield rate was observed to increase as the *pyrolysis temperature* increases from 400 °C; however, a maximum oil yield of 47.70 mass% was obtained at the *pyrolysis temperature* of 455 °C, and after this peak oil yield, there was a slight continuous gradual decline in the oil yield as the *pyrolysis temperature* further increases. This observable decline became more significant, most especially, between the *temperature* of 500 and 600 °C (Fig. 5b). It was also observed that the *temperature* range for high production of bio-oil via co-pyrolysis of a mixture of EP and RH fell within 450–550 °C. However, both the extremely high and very low *temperatures* have a negative effect on the bio-oil yield rates (Table 1). The decline in the oil yield rate at high *temperatures* could be as a result of the secondary decomposition reactions that normally occur at higher *pyrolysis temperatures* (most especially > 600 °C) during biomass thermal process during which the liquid oil is further decomposed into non-condensable gaseous products, hence a decrease in oil yield [12, 42]. Heating rate, likewise, presented a positive effect on the bio-oil yield rate (Fig. 5c). The bio-oil yield rate increases as the heating rate increases but slightly decreases, gradually, after a peak oil yield (of 47.70 mass%) was attained, at a *heating rate* of 20 °C min<sup>-1</sup> and a *temperature* of 455 °C, during the co-pyrolysis process. According to Hu et al. [12], increasing the *heating rate* from 5 to 20 °C min<sup>-1</sup>, with a *temperature* lower than 500 °C, could enhance the pyrolysis oil yield but when the treatment *temperature* exceeded 550 °C, the high heating rate of 20 °C min<sup>-1</sup> could pose a negative effect on pyrolysis oil production. This observation was also found to be consistent with the result of the effect of heating rate on the bio-oil yield rates in this present study (Fig. 5c).

In addition, the 3D surface graphs showing the interaction effects of the experimental factors on oil yield rates are presented in Fig. 5d–f. Likewise, it was also observed that the interaction effects of the RH mass percentage in the feedstock with *pyrolysis temperature* and *heating rate*, respectively, posed almost similar effects on the bio-oil yield rates when compared with their individual main effects on oil yield rates, most especially, after the peak oil yield (Fig. 5d, e). Thus, the oil yield rate was noticed to increase with an increase in the RH mass percentage in the feedstock mixture until an optimal oil peak of 47.70 mass% occurred with 80% of RH in the feedstock blend at the *heating rate* of 20 °C min<sup>-1</sup> and a *temperature* of 455 °C, respectively, after which there was observable continuous slight decline in the oil yield, even as RH mass percentage in the feedstock mixture was increased. Likewise, from Fig. 5f, it was also observed that the interaction effects of the *heating rate* and *temperature* on the bio-oil yield rates also led to an increase in the bio-oil yield provided that the *temperature* is neither extremely high nor extremely low. Similarly, a low heating rate with a low *pyrolysis temperature* treatment resulted in a low bio-oil yield rate during the fixed bed co-pyrolysis experiments (Table 2).

### The bio-char yields

The results of many studies on pyrolysis of different biomass wastes indicated that the bio-char is another vital product of the process. The regression model for the bio-char yield rate [Eq. (9)] during the co-pyrolysis process of the waste seaweed (EP) and rice husk (RH) in a fixed bed reactor was obtained according to Eq. (3). Also, the

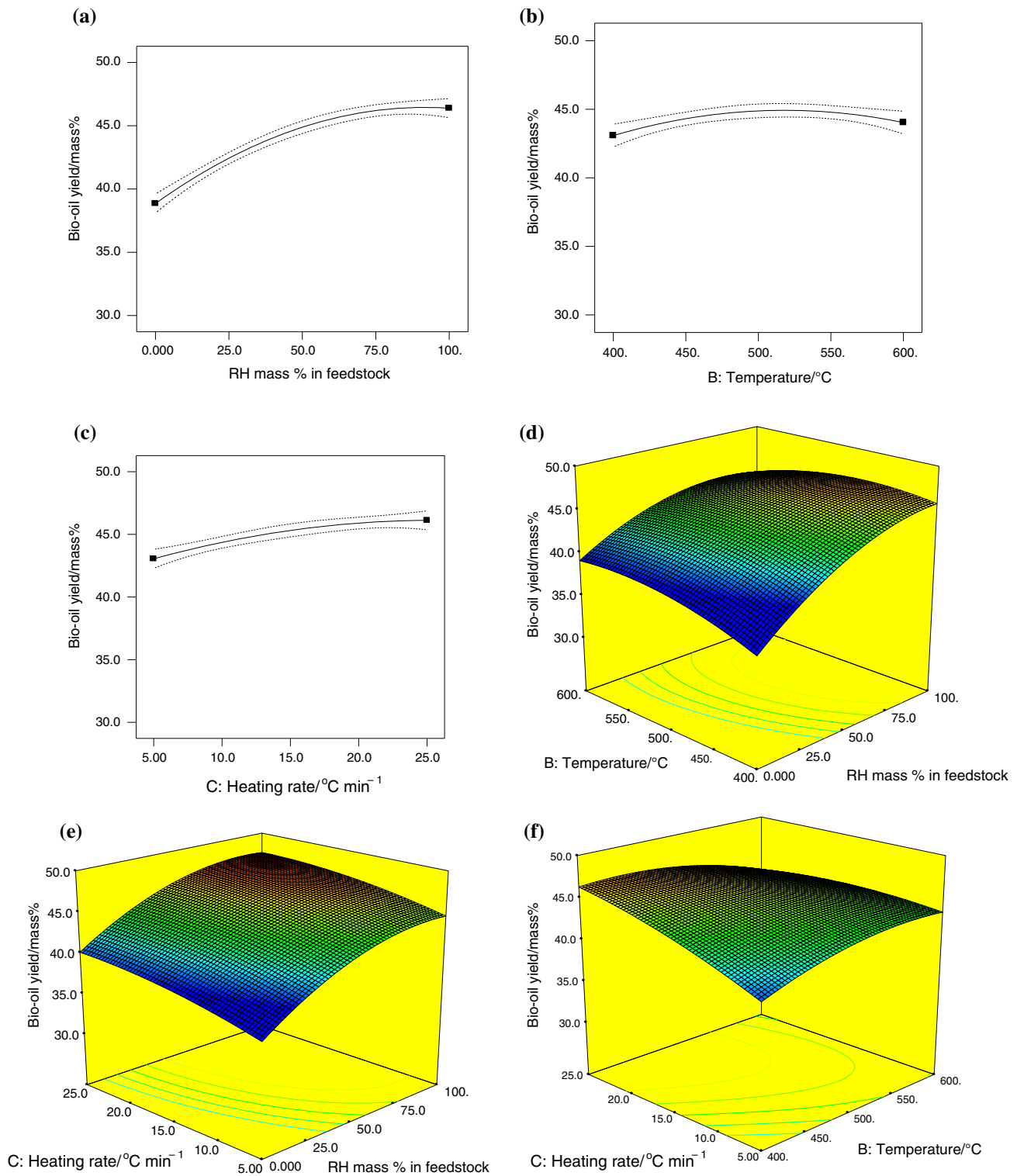


**Fig. 5** Simulated main and interaction effects of the experimental factors on the bio-oil yield rates

statistical model evaluation parameters obtained from the model ANOVA are presented in Table 4b. The fitness of the developed model is acceptable as the lack of fit was not significant ( $P > 0.05$ ). Thus, the results of the statistical

analysis revealed that all the three experimental factors influenced, greatly, the rate of production of bio-char. Figure 6 shows the main and interaction effects of the factors (i.e., the RH mass percentages in the feedstock

**Table 5** Confirmatory tests conducted in a fixed bed reactor under the same predicted optimal conditions for oil yields

Runs	Experimental factors			Bio-oil yield/mass%		Error/%
	A/%	B/°C	C/°C min <sup>-1</sup>	Actual	Predicted	
1	80	455	20	48.20	47.70	1.04
2	80	455	20	47.90	47.70	0.42
3	80	455	20	48.05	47.70	0.73

'A' represents the mass percentage of rice husk (RH) in the feedstock blend/mass%, 'B' depicts the optimal pyrolysis temperature/°C, and 'C' denotes the optimal heating rate/°C min<sup>-1</sup>

mixture, pyrolysis temperature, and heating rate) on the bio-char yield. Considering the main effects of the individual factors, it was apparently obvious that the yield of bio-char decreased with the increasing RH mass percentage in the feedstock mixture. However, it increased with the increasing mass percentage of EP in the feedstock mixture, probably because EP has higher ash content than RH (Table 1). The maximum char yield was obtained when the feedstock blend contains almost EP (Fig. 6a); however, the lowest char yield was realized at the optimal conditions (i.e., 455 °C, 20 °C min<sup>-1</sup> with 80% of RH in the blend) when the maximum oil yield was obtained during the optimization process study. It was also observed that a change in the *pyrolysis temperature* led to a slight variation in the yield of char produced. Generally, higher pyrolysis temperatures led to lower char yields owing to a better biomass conversion due to the pyrolysis primary reactions and facilitation of the secondary decomposition of char to generate non-condensable gaseous products [43, 44]. Similarly, increasing the *heating rate* lowers the amount of char produced, probably, due to the fast removal of high molecular volatiles and thus leaving lower amounts of char [45]. Thus, extremely low heating rates led to higher yields of char. Likewise, from Fig. 6, it was obvious that the interaction effects of the three experimental factors played significant roles in the amounts of char produced during the co-pyrolysis process of EP and RH. Thus, the interaction effects of the RH mass percentage in the feedstock with the *pyrolysis temperature and heating rate*, respectively, posed almost similar effects on the bio-char yield rates as the individual factors' main effects (Fig. 6a–c). It was also quite clear that higher percentages of RH in the feedstock blend led to less production of char while the reversed trend is true for the higher EP mass percentages in the mixture. Likewise, Fig 6d, 6e, and 6f presents the interaction effects of the co-pyrolysis parameters (i.e., the *RH mass percentage, temperature and heating rate*) on the char yields.

## Synergistic effect of co-pyrolysis on bio-oil yield

In order to investigate the synergistic effect of co-pyrolysis, the bio-oil yield rates were further evaluated using different biomass feed ratios (i.e., various RH mass percentages in the feedstock) at a pyrolysis temperature of 500 °C and a heating rate of 20 °C min<sup>-1</sup>. Table 6 compares the results of the observed and theoretical bio-oil yields. The theoretical values of the co-pyrolysis oil yields were estimated from the bio-oil yield rates obtained from the individual pyrolysis (at 500 °C and 20 °C min<sup>-1</sup>) of EP and RH, respectively, using Eq. (2). From Table 6, it was observed that the values of all the observed bio-oil yield rates are greater than their corresponding theoretical values, suggesting the existence of synergistic effect between EP and RH during the co-pyrolysis [12, 32, 34]. The comparison of the observed and theoretical results obtained during the co-pyrolysis revealed that an average of 2.92% increase in the total oil yield was achieved.

## Pyrolysis and co-pyrolysis products characterization

### GC/MS analysis of bio-oils from pyrolysis of EP, RH, and sample mixtures

GC–MS analysis of the bio-oils obtained from the pyrolysis experiments of EP, RH, and their sample mixtures at different feed ratios was performed in order to examine the main chemical compositions of the bio-oils. According to Aysu and Sanna [43], seaweed bio-oils, as well as those of the terrestrial plants, are very complex mixtures of organic compounds with different molecular structures and masses. They investigated the major compounds in the bio-oils from the pyrolysis of the green microalga (*Nannochloropsis*) and divided these major compounds into several groups such as aliphatics, aromatics, oxygenated compounds, nitrogen-containing compounds, and their derivatives. Zhang et al. [44] also investigated the effects of water washing and torrefaction pretreatments on rice husk pyrolysis via microwave heating, and they classified the main chemical compositions of the bio-oils into eight main groups as follows: acids, ketones/aldehydes, furans, phenols, esters, sugars, nitrogen-containing compounds, and others. In this present study, many compounds were identified in the bio-oils via GC–MS and classified into several chemical groups, based on their functional groups: furan, saccharides, phenols, aldehydes and ketones, carboxylic acids and esters, hydrocarbons, and nitrogen-containing compounds. Table 7 listed the main chemical compounds in the bio-oils as well as their relative contents, respectively, while Fig. 7 presents a summary of the

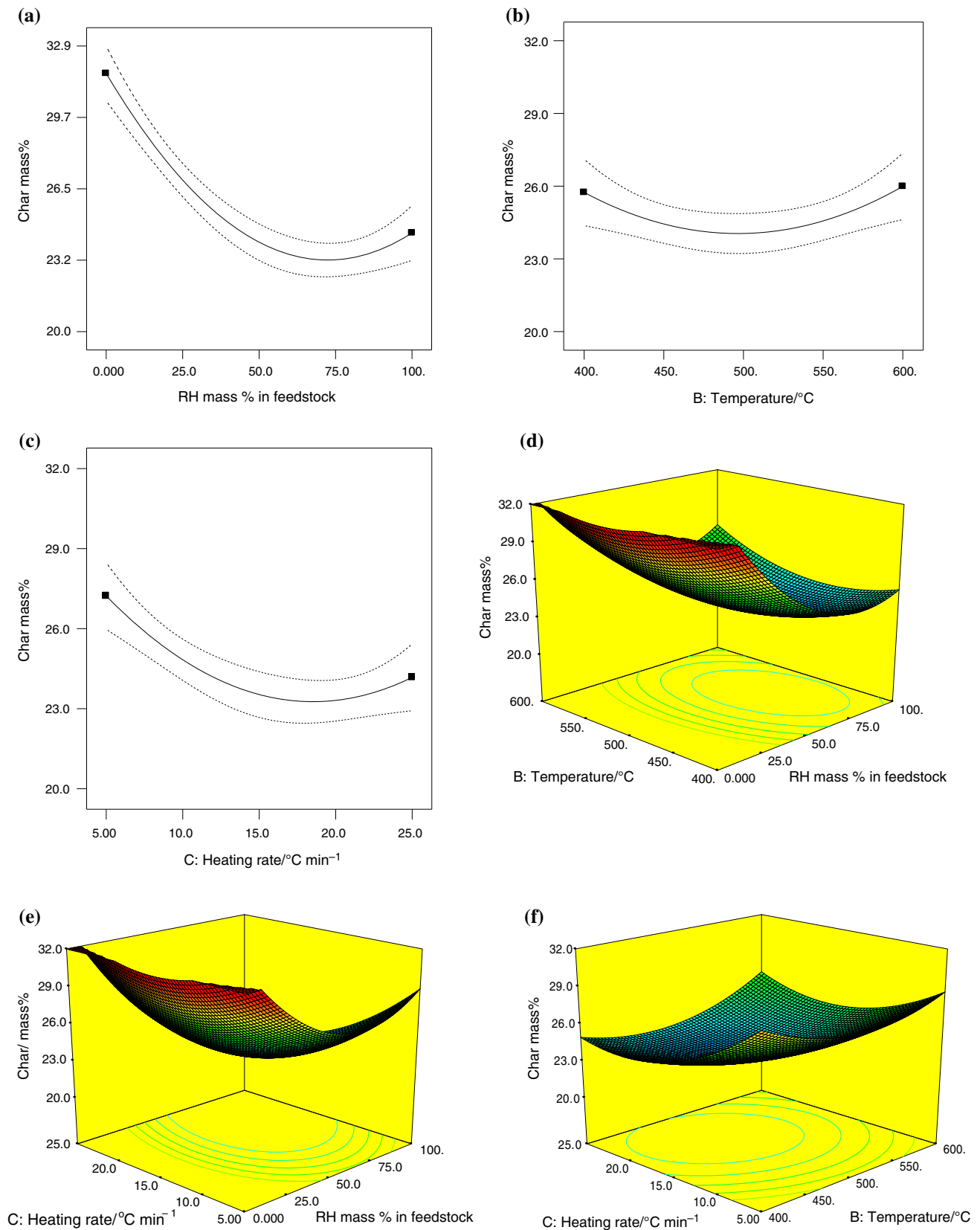


Fig. 6 Simulated main and interaction effects of the experimental factors on the char yields

**Table 6** Comparison of product yields from co-pyrolysis experiments conducted at 500 °C and 20 °C min<sup>-1</sup> with the theoretical values

RH % in the feedstock	Bio-oil yield/mass%			Char yield/mass%			Gas yield/mass%		
	Obs.	Theo.	Diff.	Obs.	Theo.	Diff.	Obs.	Theo.	Diff.
0	39.4	39.40	0	29.5	29.5	0	31.1	31.10	0
25	44.5	41.30	3.20	25.5	27.95	- 2.45	30.0	30.75	- 0.75
40	45.7	42.44	3.26	25.2	27.02	- 1.82	29.1	30.54	- 1.44
50	46.5	43.20	3.30	24.9	26.40	- 1.50	29.1	30.40	- 1.30
60	46.8	43.96	2.84	24.5	25.73	- 1.23	28.7	30.26	- 1.56
75	47.1	45.10	2.00	24.3	24.85	- 0.55	28.6	30.05	- 1.45
100	47.0	47.00	0	23.3	23.30	0	29.7	29.70	0

*Obs.* observed values, *Theo* theoretical values, *Diff.* difference between observed and theoretical values

relative compositions of the identified main group of compounds in the bio-oils. From the figure, it can be seen that the dominant compounds in the bio-oil from the pyrolysis of EP are mainly the carboxylic acids/esters (41.72%) and nitrogen-containing compounds (19.73%). Likewise, the relative contents of the bio-oils from the pyrolysis of RH as well as the sample mixtures can easily be observed directly from Fig. 7. Obviously, the GC-MS results revealed a considerable decrease in the contents of furans and saccharides in the bio-oil obtained owing to the synergistic interaction between the EP and RH during the co-pyrolysis, and an increase in the contents of the carboxylic acids and hydrocarbons, when compared with those of the EP bio-oil. These significant differences were associated with the notable role of the secondary reactions in the fixed-bed reactor or the oligomerization reaction of volatiles in condensation process [45, 46].

#### Determination of some properties of the produced bio-oil and char

Table 8 presents the *heating values* of the bio-oils and char obtained from the pyrolysis of EP, RH, and their mixtures at different blending ratios. From the table, it can be seen that the *heating values* of the bio-oils from the normal pyrolysis of EP and RH alone were 30.644 MJ kg<sup>-1</sup> and 25.501 MJ kg<sup>-1</sup>, respectively, while those of the char are 31.595 MJ kg<sup>-1</sup> and 26.878 MJ kg<sup>-1</sup>, respectively, from the individual normal pyrolysis of EP and RH. Table 8 also presents the results of the experimental heating values of the bio-oils and bio-chars from the co-pyrolysis of EP and RH at different blending ratios as well as their theoretical *heating values*, respectively, which were estimated according to the Eq. (10).

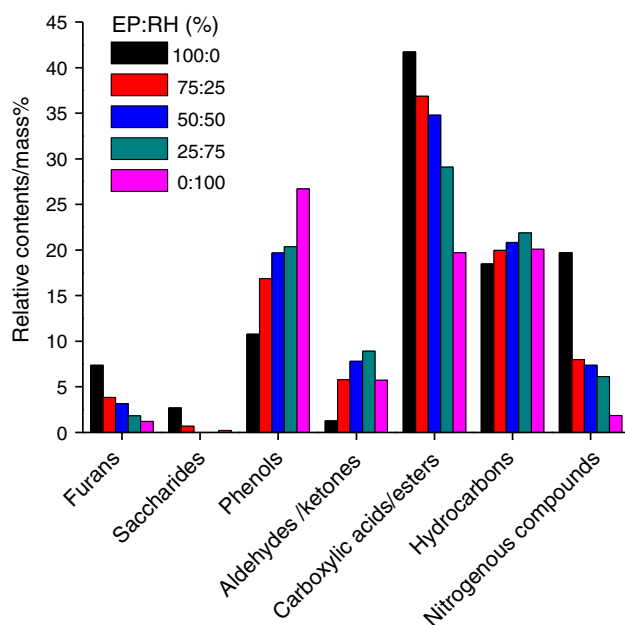
$$HHV_{\text{Theoretical}} = \omega_1 \times HHV_{\text{EP}} + \omega_2 \times HHV_{\text{RH}} \quad (10)$$

where *HHV* = *High heating value* (MJ kg<sup>-1</sup>),  $\omega_1$  and  $\omega_2$  are the feed blending ratios of EP and RH, respectively. It was observed that the experimental heating values of the bio-

oils obtained from the co-pyrolysis of the feedstock mixtures were slightly greater than the estimated theoretical values and significantly greater than that of the oil obtained from the normal pyrolysis of RH alone. This observation was similar to those of the char too. This indicates that the synergistic interaction between EP and RH during co-pyrolysis does not only have a positive effect on the bio-oil and char yields alone but also on their quality. However, the *heating value* of the 0# diesel was 46.871 MJ kg<sup>-1</sup>, which was tested in the same condition. Thus, the heating values of the bio-oils and chars were considered as low when compared to that of the conventional diesel. The low heating value of the bio-oils was associated with the presence of the oxygenate compounds (phenols, furans, ketones, aldehydes, carboxylic acids, and monosaccharides), and this also makes the bio-oil unstable and lowers its miscibility with hydrocarbons [47]. There is, thus, an essential need for catalytic co-pyrolysis of EP and RH for the production of bio-oils of higher grade or co-pyrolysis of a mixture of EP and RH with polymers, to further enhance the heating values and other essential properties of the resultant co-pyrolysis products. This briefly defines our next course of research. Other physical properties of the bio-oils such as the specific gravity and moisture content were measured accordingly and are also presented in Table 8. It can also be observed from the table that bio-oils with different specific gravities were obtained from the pyrolysis of EP (seaweed), RH (rice husk), and their mixtures at different blending ratios, respectively. Similar results have been obtained by many researchers. For instance, Bakar and Titiloye [23] obtained bio-oil with a specific gravity of 1.065 from rice husk pyrolysis, Ji-lu [48] got bio-oil with a specific gravity of 1.190 and water content of 25.2 mass%, Lu et al. [49] obtained 1.140 with a water content of 28 mass%, while Tsai et al. [24] got 1.210 with a moisture content 33.80 mass% from rice husk. Likewise, Bae et al. [50] achieved maximum bio-oil yields of 39.50 mass% and 47.4 mass% with water contents of 37.50 mass% and 44.7 mass%, respectively, from

**Table 7** Main chemical compositions of the bio-oil from different feedstock blending ratios via GC–MS analysis

Groups	Major compounds	Relative contents of the bio-oils/mass%				
		100:0	75:25	50:50	25:75	0:100
Furans	Furan	2.76	1.96	1.52	0.77	0.30
	Furaltadone	1.26	–	–	–	0.58
	Furan, tetrahydro	3.34	1.89	1.63	1.06	0.82
Saccharides	L-Glucose, 6-deoxy	2.69	0.33	–	–	0.21
Phenols	Phenol	4.05	5.86	7.20	7.48	8.85
	Phenol, 3-methyl	4.99	5.32	5.70	5.99	7.63
	Phenol, 4-ethyl	1.73	4.58	4.98	5.03	6.48
	Phenol, 2-methoxy	–	1.10	1.80	1.87	3.76
Aldehydes/ketones	Benzofuran	1.26	5.79	7.8	8.91	5.73
Carboxylic acids/esters	Acetic acid	13.1	14.98	13.87	9.75	4.78
	Propanoic acid	3.28	3.21	3.18	3.02	2.39
	Propenoic acid	3.63	5.13	4.79	4.06	0.35
	Butyrolactone	6.67	–	–	–	4.88
	Formic acid, ethenyl ester	5.26	5.12	5.04	5.11	3.39
	n-Hexadecanoic acid	9.78	8.43	7.91	7.15	3.93
Hydrocarbons	Propane	0.81	16.98	17.75	17.84	17.49
	Propene	2.72	2.97	3.08	4.03	0.48
	Cyclopropene	14.94	–	–	–	2.11
Nitrogen-containing compounds	Pyridine, 3-methyl	5.43	1.34	1.05	0.65	0.25
	2(1H)-Pyridinone	5.95	4.99	4.87	4.26	1.15
	Acetamide	3.42	1.67	1.46	1.21	0.45
	Indole	4.93	–	–	–	–

**Fig. 7** Relative contents of the main compositions in the bio-oils from different feedstock ratios

pyrolysis of two brown macroalgae (*Undaria pinnatifida* and *Laminaria japonica*) at the optimal temperature of 500 °C. Thus, the results of the determined oil properties

revealed that co-pyrolysis could also improve the oil quality, besides the increment in the oil yield. The results of the ultimate analysis of the bio-oils and char products from the pyrolysis of EP alone, RH alone, and their blends at different feed ratios are also presented in Table 8.

## Conclusions

Pyrolysis of EP and RH in a fixed-bed reactor has been investigated. Production of bio-oil and char from the co-pyrolysis was optimized. Operating variables (i.e., the feedstock blending ratio, pyrolysis temperature, and heating rate) were studied using a central composite circumscribed design. The effects and significance of the developed models on the responses were evaluated using analysis of variance, model evaluation statistical parameters, and response surface curves. The maximum pyrolysis oil was obtained at the optimal conditions of 455 °C and 20 °C min<sup>-1</sup> with 80% mass of RH in the mixture. The pyrolysis products' analysis results unveiled that synergistic effect exists between EP and RH during the process, and this led to the production of improved co-pyrolysis products.

**Table 8** Properties of pyrolysis products from co-pyrolysis experiments performed at heating rate of 20 °C min<sup>-1</sup> and a temperature of 500 °C

Properties	Values				
	0	25	50	75	100
<i>Bio-oil</i>					
Moisture content/mass%	25.48	26.36	27.27	27.96	28.64
Specific gravity	1.018	1.021	1.032	1.044	1.059
Elemental composition/mass%					
C	51.40	49.16	47.94	45.37	42.81
H	5.17	6.49	6.83	7.09	7.86
O <sup>a</sup>	39.28	41.38	43.19	45.96	48.83
N	4.15	2.97	2.04	1.58	0.50
H/C ratio	1.21	1.58	1.71	1.86	2.20
Experimental HHV/MJ kg <sup>-1</sup>	30.644	29.875	28.974	26.987	25.501
Theoretical HHV/MJ kg <sup>-1</sup>	30.644	29.35825	28.0725	26.78675	25.501
<i>Char</i>					
Elemental composition/mass%					
C	52.72	50.07	48.06	46.43	45.93
H	4.93	5.97	6.59	6.90	6.98
O <sup>a</sup>	37.15	39.09	42.84	44.75	45.99
N	5.20	4.87	2.51	1.92	1.10
H/C ratio	1.12	1.43	1.65	1.78	1.82
Experimental HHV/MJ kg <sup>-1</sup>	31.595	30.984	29.825	28.683	26.878
Theoretical HHV/MJ kg <sup>-1</sup>	31.595	30.41575	29.2365	28.05725	26.878

<sup>a</sup>Calculated by difference

**Acknowledgements** This work was supported by the National Natural Science Funds Fund of China (No. 51676091), the China Postdoctoral Science Foundation (No. 2018M630529), the Jiangsu Province ‘333’ Project (2018), and the Six Talent Peaks Project in Jiangsu Province (2018).

## References

- Wang S, Hu Y, Wang Q, Xu S, Lin X, Ji H, Zhang Z. TG–FTIR–MS analysis of the pyrolysis of blended seaweed and rice husk. *J Therm Anal Calorim.* 2016;126(3):1689–702.
- Filipe P, Filomena P, Ibrahim G, Isabel C, Nuno L. Study of the co-pyrolysis of biomass and plastic wastes. *Clean Technol Environ.* 2009;11:115–22.
- Wang SR, Dai GX, Yang HP, Luo ZY. Lignocellulosic biomass pyrolysis mechanism: a state of-the-art review. *Prog Energy Combust Sci.* 2017;62:33–86.
- John RP, Anisha GS, Nampoothiri KM, Pandey A. Micro and macroalgal biomass: a renewable source for bioethanol. *Bioresour Technol.* 2011;102:186–93.
- Abnisa F, Daud WMAW. A review on co-pyrolysis of biomass: an optional technique to obtain a high-grade pyrolysis oil. *Energy Convers Manage.* 2014;87:71–85.
- Singh J, Gu S. Commercialization potential of microalgae for biofuels production. *Renew Sustain Energy Rev.* 2010;14(9):2596–610.
- Wei N, Quarterman J, Jin YS. Marine macroalgae: an untapped resource for producing fuels and chemicals. *Trends Biotechnol.* 2013;31:70–7.
- Gao K, Mckinley KR, Gao SK. Use of macroalgae for marine biomass production and CO<sub>2</sub> remediation: a review. *J Appl Phycol.* 1994;6:45–60.
- Zhang DH, Wang JQ, Lin YG, Si YL, Huang C, Yang J, Huang B, Li W. Present situation and future prospect of renewable energy in China. *Renew Sustain Energy Rev.* 2017;76:865–71.
- Wang S, Hu Y, Uzoejinwa BB, Cao B, He Z, Wang Q, Xu S. Pyrolysis mechanisms of typical seaweed polysaccharides. *J Anal Appl Pyrol.* 2017;124:373–83.
- Yang HP, Yan R, Chen HP, Lee DH, Zheng CG. Characteristics of hemicellulose, cellulose and lignin pyrolysis. *Fuel.* 2007;86:1781.
- Hu G, Li J, Zhang X, Li Y. Investigation of waste biomass co-pyrolysis with petroleum sludge using a response surface methodology. *J Environ Manage.* 2017;192:234–42.
- Alvarez J, Lopez G, Amutio M, Bilbao J, Olazar M. Bio-oil production from rice husk fast pyrolysis in a conical spouted bed reactor. *Fuel.* 2014;128:162–9.
- Quan C, Xu S, An Y, Liu X. Co-pyrolysis of biomass and coal blend by TG and in a free fall reactor. *J Therm Anal Calorim.* 2014;117(2):817–23.
- Choi J, Choi JW, Suh DJ, Ha JM, Hwang JW, Jung HW, Lee KY, Woo HC. Production of brown algae pyrolysis oils for liquid biofuels depending on the chemical pretreatment methods. *Energy Convers Manage.* 2014;86:371–8.
- Harun R, Danquah MK, Forde GM. Microalgal biomass as a fermentation feedstock for bioethanol production. *J Chem Technol Biotechnol.* 2010;85(2):199–203.
- Kim NJ, Li H, Jung K, Chang HN, Lee PC. Ethanol production from marine algal hydrolysates using *Escherichia coli* KO11. *Bioresour Technol.* 2011;102(16):7466–9.

18. Wang SR, Ru B, Dai GX, Lin HZ, Zhang L. Influence mechanism of torrefaction on softwood pyrolysis based on structural analysis and kinetic modeling. *Int J Hydrog Energy*. 2016;41:1642–8.
19. Ross AB, Anastasakis K, Kubacki M, Jones JM. Investigation of the pyrolysis behaviour of brown algae before and after pretreatment using PY-GC/MS and TGA. *J Anal Appl Pyrol*. 2009;85:3–10.
20. Ross AB, Jones JM, Kubacki ML, Bridgeman T. Classification of macroalgae as fuel and its thermochemical behavior. *Bioresour Technol*. 2008;99:6494–504.
21. Wang S, Jiang XM, Wang N, Yu LJ, Li Z, He PM. Research on pyrolysis characteristics of seaweed. *Energy Fuels*. 2007;21:3723–9.
22. Hu ZQ, Zheng Y, Yan F, Xiao B, Liu S. Bio-oil production through pyrolysis of blue-green algae blooms (BGAB): product distribution and bio-oil characterization. *Energy*. 2013;52:119–25.
23. Bakar MSA, Titiloye JO. Catalytic pyrolysis of rice husk for bio-oil production. *J Anal Appl Pyrol*. 2013;103:362–8.
24. Tsai WT, Lee MK, Chang YM. Fast pyrolysis of rice husk: product yields and compositions. *Bioresour Technol*. 2007;98:22–8.
25. Zheng JL. Bio-oil from fast pyrolysis of rice husk: yields and related properties and improvement of the pyrolysis system. *J Anal Appl Pyrol*. 2007;80:30–5.
26. Uzunov I, Uzunova S, Angelova D, Gigova A. Effects of the pyrolysis process on the oil sorption capacity of rice husk. *J Anal Appl Pyrol*. 2012;98:166–76.
27. Wang S, Jiang XM, Han XX, Wang H. Fusion characteristic study on seaweed biomass ash. *Energy Fuels*. 2008;22:2229–35.
28. Li DM, Chen LM, Chen SL, Chen S, Zhang X, Chen F, Ye N. Comparative evaluation of the pyrolytic and kinetic characteristics of a macroalga (*Sargassum thunbergii*) and a freshwater plant (*Potamogeton crispus*). *Fuel*. 2012;96:185–91.
29. Li SD, Chen XL, Liu AB, Wang L, Yu GS. Study on co-pyrolysis characteristics of rice straw and Shenfu bituminous coal blends in a fixed bed reactor. *Bioresour Technol*. 2014;155:252–7.
30. Isahak WNRW, Hisham MWM, Yarmo MA, Hin TY. A review on bio-oil production from biomass by using pyrolysis method. *Renew Sustain Energy Rev*. 2012;16:5910–23.
31. Kuppens T, Cornelissen T, Carleer R, Yperman J, Schreurs S, Jans M, et al. Economic assessment of flash co-pyrolysis of short rotation coppice and biopolymer waste streams. *J Environ Manag*. 2010;91:2736–47.
32. Önal E, Uzun BB, Pütün AE. Bio-oil production via co-pyrolysis of almond shell as biomass and high density polyethylene. *Energy Convers Manage*. 2014;78:704–10.
33. Mei-Yu H, Bao-Xia L. Co-pyrolysis characteristics of the sugarcane bagasse and *Enteromorpha prolifera*. *Energy Convers Manage*. 2016;120:238–46.
34. Abnisa F, Daud WMAW, Ramalingam S, Naquuddin M, Azemi BM, Sahu JN. Co-pyrolysis of palm shell and polystyrene waste mixtures to synthesis liquid fuel. *Fuel*. 2013;108:311–8.
35. Martinez JD, Veses A, Mastral AM, Murillo R, Navarro MV, Puy N, et al. Co-pyrolysis of biomass with waste tyres: upgrading of liquid bio-fuel. *Fuel Process Technol*. 2013;119:263–71.
36. Brebu M, Ucar S, Vasile C, Yanik J. Co-pyrolysis of pine cone with synthetic polymers. *Fuel*. 2010;89:1911–8.
37. Samanya J, Hornung A, Apfelbacher A, Vale P. Characteristics of the upper phase of bio-oil obtained from co-pyrolysis of sewage sludge with wood, rapeseed and straw. *J Anal Appl Pyrol*. 2012;94:120–5.
38. Wang J, Wang GC, Zhang MX, Chen M, Li D, Min F, Chen M, Zhang S, Ren Z, Yan Y. A comparative study of thermolysis characteristics and kinetics of seaweeds and fir wood. *Process Biochem*. 2006;41:1883–6.
39. Yi S, Su Y, Qia B, Su Z, Wan Y. Application of response surface methodology and central composite rotatable design in optimizing the preparation conditions of vinyltriethoxysilane modified silicalite/polydimethylsiloxane hybrid pervaporation membranes. *Sep Purif Technol*. 2010;71:252–62.
40. Idris A, Kormin F, Noordin MY. Application of response surface methodology in describing the performance of thin film composite membrane. *Sep Purif Technol*. 2006;49:271–80.
41. Wang S, Wang Q, Jiang XM, Han X, Ji H. Compositional analysis of bio-oil derived from pyrolysis of seaweed. *Energy Convers Manage*. 2013;68:273–80.
42. Shen DK, Gu S, Luo KH, Bridgwater AV, Fang MX. Kinetic study on thermal decomposition of woods in oxidative environment. *Fuel*. 2009;88(6):1024–30.
43. Aysu T, Sanna A. Nannochloropsis algae pyrolysis with ceria-based catalysts for production of high-quality bio-oils. *Bioresour Technol*. 2015;194:108–16.
44. Zhang S, Dong Q, Zhang L, Xiong Y, Liu X, Zhu S. Effects of water washing and torrefaction pretreatments on rice husk pyrolysis by microwave heating. *Bioresour Technol*. 2015;193:442–8.
45. Butler E, Devlin G, Meier D, McDonnell K. Fluidised bed pyrolysis of lignocellulosic biomasses and comparison of bio-oil and micropyrolyser pyrolysate by GC/MS-FID. *J Anal Appl Pyrol*. 2013;103:96–101.
46. Patwardhan PR, Dalluge DL, Shank BH, Brown RC. Distinguishing primary and secondary reactions of cellulose pyrolysis. *Bioresour Technol*. 2011;102(8):5265–9.
47. Bridgwater AV. Review of fast pyrolysis of biomass and product upgrading. *Biomass Bioenergy*. 2012;38:68–94.
48. Ji-lu Z. Bio-oil from fast pyrolysis of rice husk: yields and related properties and improvement of the pyrolysis system. *J Anal Appl Pyrol*. 2007;80:30–5.
49. Lu Q, Xu-lai Y, Xi-feng Z. Analysis on chemical and physical properties of bio-oil pyrolyzed from rice husk. *J Anal Appl Pyrol*. 2008;82:191–8.
50. Bae YJ, Ryu C, Jeon JK, Park JK, Suh DJ, Suh YW, Chang D, Park YK. The characteristics of bio-oil produced from the pyrolysis of three marine macroalgae. *Bioresour Technol*. 2011;102:3512–20.